DESIGNING GREEN STORMWATER INFRASTRUCTURE FOR HYDROLOGIC AND HUMAN BENEFITS: AN IMAGE BASED MACHINE LEARNING APPROACH

BY

ANKIT RAI

THESIS

Submitted in partial fulfillment of the requirements
for the degree of Master of Science in Civil Engineering
in the Graduate College of the
University of Illinois at Urbana-Champaign, 2013

Urbana, Illinois

Adviser:

Professor Barbara Minsker

ABSTRACT

Urbanization over the last century has degraded our natural water resources by increasing storm-water runoff, reducing nutrient retention, and creating poor ecosystem health downstream. The loss of tree canopy and expansion of impervious area and storm sewer systems have significantly decreased infiltration and evapotranspiration, increased stream-flow velocities, and increased flood risk. These problems have brought increasing attention to catchment-wide implementation of green infrastructure (e.g., decentralized green storm water management practices such as bioswales, rain gardens, permeable pavements, tree box filters, cisterns, urban wetlands, urban forests, stream buffers, and green roofs) to replace or supplement conventional storm water management practices and create more sustainable urban water systems. Current green infrastructure (GI) practice aims at mitigating the negative effects of urbanization by restoring pre-development hydrology and ultimately addressing water quality issues at an urban catchment scale. The benefits of green infrastructure extend well beyond local storm water management, as urban green spaces are also major contributors to human health. Considerable research in the psychological sciences have shown significant human health benefits from appropriately designed green spaces, yet impacts on human wellbeing have not yet been formally considered in GI design frameworks. This research develops a novel computational green infrastructure (GI) design framework that integrates storm water management requirements with criteria for human wellbeing. A supervised machine learning model is created to identify specific patterns in urban green spaces that promote human wellbeing; the model is linked to RHESSYS hydrological model to evaluate GI designs in terms of both water resource and human health benefits. An application of the models to Dead Run Watershed in Baltimore showed that image mining

methods were able to capture key elements of human preferences that could improve tree-based GI design. Hydrologic benefits associated with these features were substantial, indicating that increased urban tree coverage and a more integrated GI design approach can significantly increase both human and hydrologic benefits.

ACKNOWLEDGEMENTS

First and foremost, I would like to thank my adviser, Professor Barbara Minsker for giving me this exciting and challenging project. Throughout the last two years, she has been constant source of inspiration, guidance, and support. I would like to express my gratitude and respect for my adviser.

I take this opportunity to thank Professor William Sullivan, from the Department of landscape and Architecture, for providing the training data for human preference ratings from his ongoing research, without which this research would not have been possible.

This work would not have been possible without the hydrologic data provided by Professor Larry Band, at the University of North Carolina, Chapel Hill. I would also like to express my sincere thanks to Taehee Hwang, Post-doctoral student at UNC, Chapel Hill for assisting me with RHESSYS modeling.

Thanks also to those; I have had the privileged of working with at UNC, Chapel Hill and RENCI. Much of my understanding of RHESSYS modeling has been gained through interacting with them during the event of WSSI hackanthon.

I've had privileged of working with the most intellectual and enthusiastic research group - EISA (Environmental Informatics & Systems Analysis). I want to thank to all members of Professor Minsker Research group for all intellectual discussions and ideas we shared this last two years. I have indeed been very lucky to interact with such bright and wonderful people.

Finally, I would like to take this opportunity to thank my parents for their immense support, care, affection, encouragement, my sister for always being there for support, my friends for their love

and affection, my maternal grandmother for her blessings, and my Grandparents, who if were here today would have been the happiest of all from my achievement.

Contents

Chapter 1

Introduction & Motivation

The rapid growth of urbanization interferes with natural water and nutrient cycling by increasing impervious surfaces, which in turn increases flashiness of urban drainage systems and reduces water quality, causing human health and ecosystem problems downstream (NRC, 2008; Wendel et al., 2011). This problem has increased interest in using green infrastructure (bioswales, rain gardens, permeable pavements, tree box filter, cisterns, urban wetlands, green roofs, etc.) as a best management practice for capturing storm-water and thereby filtering pollutants and slowing flows (Dietz, 2007). Poff et al. (1997) suggested that implementation of these practices at the watershed scale should restore the riverine ecosystem along with addressing water quality issues. Furthermore, Roy et al. (2008) considered watershed-wide implementation of these approaches as a prerequisite for sustainable urban water systems.

Currently, green infrastructure design guidelines provide site-specific (patch) criteria with only qualitative discussion of catchment-scale impacts of GI installations (e.g, CalTrans (2010); City of Portland (2008); Harper and Baker (2007); MDE (2009); NCDWQ (2007). Catchment-scale lumped-parameter stormwater models (e.g., MARC (2008); Vassilios et al. (1997); and tools such as HSPF, SWMM and HEC–HMS) do not represent site-specific hydrology or GI processes. In these catchment-scale models, both traditional ("grey") and green infrastructure have typically been modeled as "edge-of-field" or "in-line" filters and sinks for storm-water runoff received from source catchment areas. Attenuation of storm-water volumes and pollutants are often included as fixed reduction percentages or first-order decay reactions based on limited input and output water quality measurements (e.g., Lee et al. (2012), in the SUSTAIN modeling framework, and Wong et al. (2001), in the MUSIC framework).

Research over the past decade as part of the Baltimore Ecosystem Study suggests that significant carbon sequestration and nitrogen retention can occur in a range of urban ecosystem features, including lawns, gardens, and stormwater detention structures, but that these processes are sensitive to specific characteristics of the integrated drainage system, including contributing areas, flow regimes, soils, and structure design (e.g. Raciti et al. (2011a,b); Bettez and Groffman (2012)). Living components of green infrastructure will grow and adjust to prevailing water, climate, and nutrient conditions, and there may be a long, transient development of ecosystem cycling and retention capacity following development. Design of sustainable green infrastructure as either edge-of-field or at-source treatment should incorporate transient development as the ecosystem develops in response to local climate, soil, and drainage position (e.g. location within a flow field). It is critical that GI modeling extend to encompass the full catchment as a continuum beyond the discrete GI sites, including runoff source areas in addition to edge-of-field or in-line treatment systems.

Furthermore, the benefits of green infrastructure extend well beyond local storm water control, as urban green spaces (e.g., lakes, parks, and community gardens) are also major contributors both to the quality of the urban ecosystem and to human health (Morris (2003); NRC (2008); and Wendel et al. (2011)). Good quality green spaces encourage people to walk, run, cycle, play and engage in many other recreational activities that provide opportunities for healthy physical activity and reduce mental stress (Douglas, 2004). According to Ulrich (1984), outdoor activities in such environments allow our sensory apparatus to relax and recover from stress. Green spaces also improve air quality, reduce noise pollution, filter out air-borne dust and contaminants, and can partially offset greenhouse gas emissions (Dunn (2010); Pataki et al.

(2011); Pincetl (2007)). A wide range of water and nutrient capture activity by natural and quasi-natural green environments contribute to human wellbeing.

The human health benefits (co-benefits) of urban green spaces have been well studied and documented in physiological as well as psychological sciences (Kuo & Sullivan (2001a)). Forty years of research has established the powerful and consistent effects of the presence of natural elements in increasing human preferences for urban landscapes (Kaplan & Kaplan (1989)). These high-preference elements, in turn, are now associated with a variety of health benefits including faster recover from stressful experiences, reduced physiological symptoms of stress (Thompson, et al. (2012); Chang & Chen (2005)), and increased life expectancy after controlling for a host of features associated with mortality (Mitchell & Popham (2008); Takano, et al. (2002)).

Despite all these benefits, green infrastructure (GI) design has not yet considered criteria for human wellbeing, at least not in any formal design structure. Along with the storm water management requirements there is a need to quantify the significance of candidate GI designs for human wellbeing. In this research we propose a new design framework that considers both human benefits of GI. To aid in rapid initial evaluation of potential GI designs, we have developed a human preference model that predicts human benefits of GI using supervised machine learning algorithms and computer vision techniques. The model is validated using data from a study in Galesburg, IL. The resulting algorithm is then coupled with a hydrologic model called RHESSYS to estimate human benefits for a GI design case study in Baltimore, MD. To our best knowledge this is the first study that quantifies the significance of urban green infrastructure design for both human wellbeing and hydrologic benefits.

Chapter 2

Methodology

This section presents the fundamental concepts and technologies used to create a GI design framework that integrates human preferences for green spaces, which are correlated with human health benefits, and hydrologic benefits.

An overview of the green infrastructure design framework is given in Figure 1. In order to predict GI human benefits, an image-based machine learning approach (presented in Section 2.1) is used to visually identify certain landscape features in design images that humans prefer, and are therefore linked with improved human health (Sullivan et.al, 2004), and provide a quantitative ranking of the design. To link these human preference criteria with storm water requirements, RHESSYS (Tague and Band, 2004) is used to predict hydrologic benefits of the design's landscape features, as described in Section 2.2.

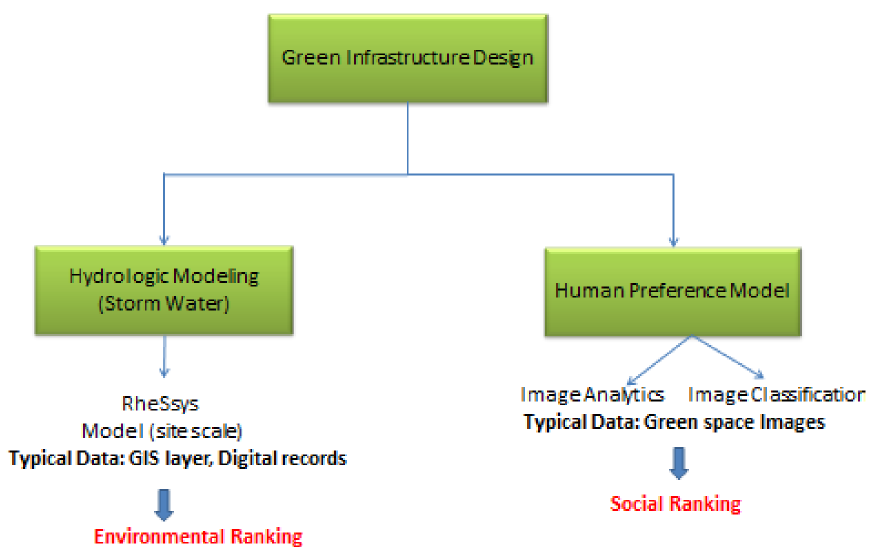

Figure 1: Green infrastructure design framework.

2.1 An image-based machine learning model to predict human preference ratings for GI designs:

Ongoing and previous research has shown that preferences of stakeholders can be predicted using digital images which visually represent potential GI designs (Sullivan, Anderson, & Lovell, 2004). For example, Figure 2 shows GI design images from Galesburg, Illinois, described in more detail in Section 3, and their human preference rankings. In order to use these types of data for predicting human health benefits of GI designs, an image-based supervised machine learning approach is developed, shown in Figure 3. The approach automates the prediction of human preferences from GI design images by identifying (extracting) landscape features that correlate with high human preferences (Kaplan & Kaplan, 1989) using computer vision techniques (see Figure 2). A supervised machine learning model is then trained to predict a human preference rating for the image based on the extracted features. Section 2.1.1 gives the features that were selected to represent the link between GI designs and human preferences, as well as an overview of the methods used to extract those features. Sections 2.1.2 through 2.1.5 provide more details on each feature extraction method. Finally, Section 2.1.6 presents the supervised machine learning model used to predict human preferences from these extracted image features.

(a) A low preference setting (b) A high preference setting

Figure 2: Sample GI design settings in Galeburg, IL (Sullivan, et. al).

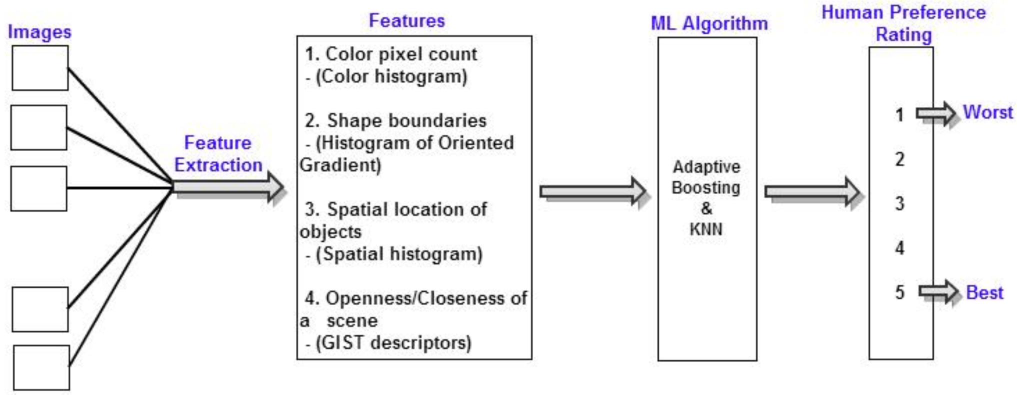

Figure 3: Stages in the image-based human preference model for GI design infrastructure.

2.1.1. Feature Extraction:

Figure 4 shows a typical green space image, marked with examples of the types of features that can be extracted and correlated with human preference rankings.

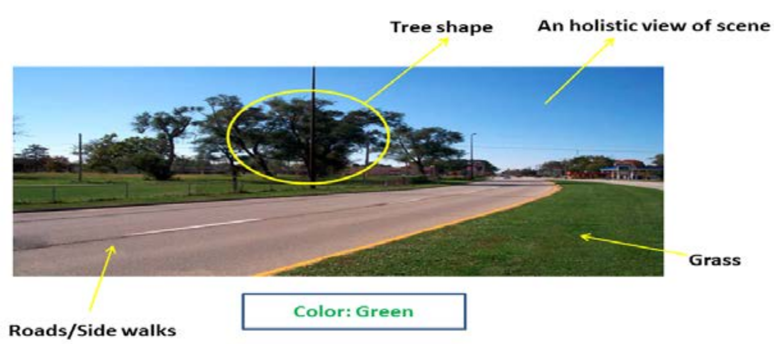

Figure 4: Typical features that can be extracted from GI design images.

To identify which image features to include in the model, Table 1 maps available image segmentation algorithms to the human preference matrix developed by Kaplan and Kaplan (1989) for urban green spaces, which gives GI characteristics that are most linked to human wellbeing. The column on the left gives landscape features that attract people and engage them longer by promoting human understanding, while the column on the right are features that encourage human exploration of the landscape. Entries in the table give the landscape features from Kaplan and Kaplan (1989) that most correlate with human wellbeing and image segmentation algorithms that can extract these types of features from design images. These features and algorithms are defined in more detail below.

Table 1: Preference Matrix

Understanding	**Exploration**
Coherence Color histogram identifies green shapes and their layouts.	*Complexity* GIST descriptor identifies openness.
Legibility EOH identifies distinctive shapes of trees and pathways.	*Mystery* Spatial histogram identifies spatial locations of features (e.g., paths partially hidden by trees) and GIST descriptor identifies their openness.

- **Coherence:** How clear and orderly the green setting appears.
- **Complexity**: The richness and variety in visual components of the setting that encourage exploration.
- **Legibility:** The distinctiveness of the setting.
- **Mystery:** The extent to which features are partially hidden from view (e.g., via curving pathways), which encourages exploration.

The feature extraction algorithms that are used to identify these characteristics in GI design images are listed as follows, and described in more detail in Sections 2.1.2 through 2.1.5: (1) color histogram identifies color features in the GI image (Vailaya et al., 1998); (2) edge orientation histogram (EOH) identifies object shapes and boundaries, such as trees and paths (Dalal et al., 2007; (3) spatial histogram extracts the spatial location of objects in the image (Birchfield and Rangarajan, 2005); and (4) GIST descriptor identifies low-dimensional features of the scene representing openness, closeness, naturalness, and roughness in GI images (Oliva and Torralba , 2001).

2.1.2 Color Histogram:

Color histograms are used for identifying color features for image classification (Anami, et.al, 2010). The color green is an important feature in GI design, therefore color-based segmentation algorithm (Wu, et.al., 2007) is implemented to compute the amount of green color intensity in an image. The key concept of color-based segmentation is to separate an object of a particular color in an image from other objects. The separation of objects is performed using unsupervised clustering analysis, which is the process of finding subsets of data points with maximum similarity (Hartigan, 1975). In this research, k-means clustering (McQueen, 1967) is implemented as a color-based segmentation algorithm using Matlab. The first step involves converting an RGB (Red, Blue, and Green added together in a color space to produce a broad array of colors) input image to an L*a*b* color space. A color space is an abstract mathematical model that describes the way colors can be represented as tuples of numbers. The L*a*b* color space consists of a luminosity layer 'L*', chromaticity layer 'a*', which decides where color falls along red-green axes, and chromaticity layer 'b*, which indicates where color falls along blue-yellow axes. The L*a*b* color space is used to quantify visual differences. Next, the objects in the L*a*b* image are clustered using K-means clustering, labeled with a unique cluster-index, and separated based on the value of k (number of specified cluster).

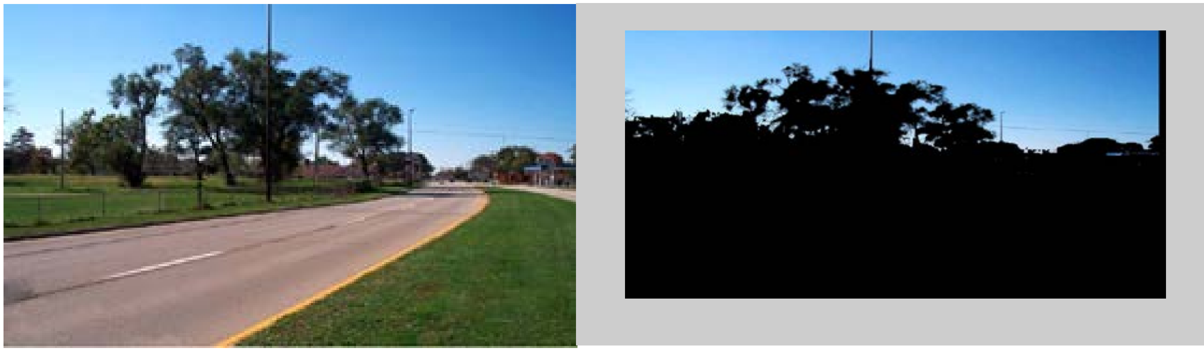

Figure 5: Color-based segmentation using k-means clustering.

Figure 5 shows a sample image of a color-based segmentation result from k-means clustering. For k=2 clusters, the algorithm separates the sky from the landscape features, including pavements and green features. This segmented image is then used to compute the color histogram that gives the color distribution of pixels in the image (Anami, et.al, 2010), as shown in Figure 6. Since color is not uniform in the image, the segmented images from k-means clustering are first converted into HSV color space. In HSV color space, H is the hue which describes the actual wavelength of color; it makes the green color distinguishable. After the image is converted to HSV color space, the color histogram is computed by counting the number of pixels of each color as shown in Figure 6; each bin represents one color intensity.

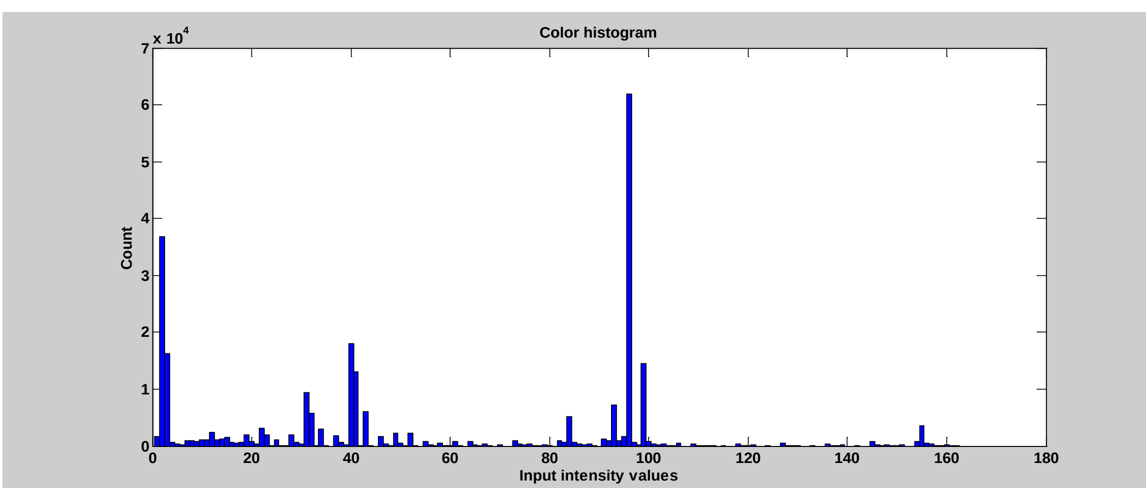

Figure 6: Color histogram.

2.1.3 Edge Orientation Histogram (EOH):

The edge orientation histogram is used to extract the distribution of edges of objects in an image (Dalal et al., (2005)). The distribution of edges is a good image feature to help with finding the distinctive shapes of objects present in a design image (e.g., the shapes of trees shown in Figure 3), which are needed to determine the legibility feature in Table 1 that affects human understanding of the scene. The first step in computing the EOH is to identify the edges in each input image. Canny edge detector is an edge detection operator that detects a wide range of edges in images. It takes a gray-scale image (where colors are converted to shades of gray) as input, and produces as output an image showing the positions of tracked pixel intensity discontinuities. Figure 6 shows the edge segmented image using canny edge operator on the gray-scale image of the landscape shown in Figure 4. The edges of the resulting image are then categorized into five classes that identify their direction: vertical, horizontal, 450-diagonal, 1350-diagonal, and isotropic. The classes are chosen based on the steepness of slope at each pixel (Anami et. al, (2010)).

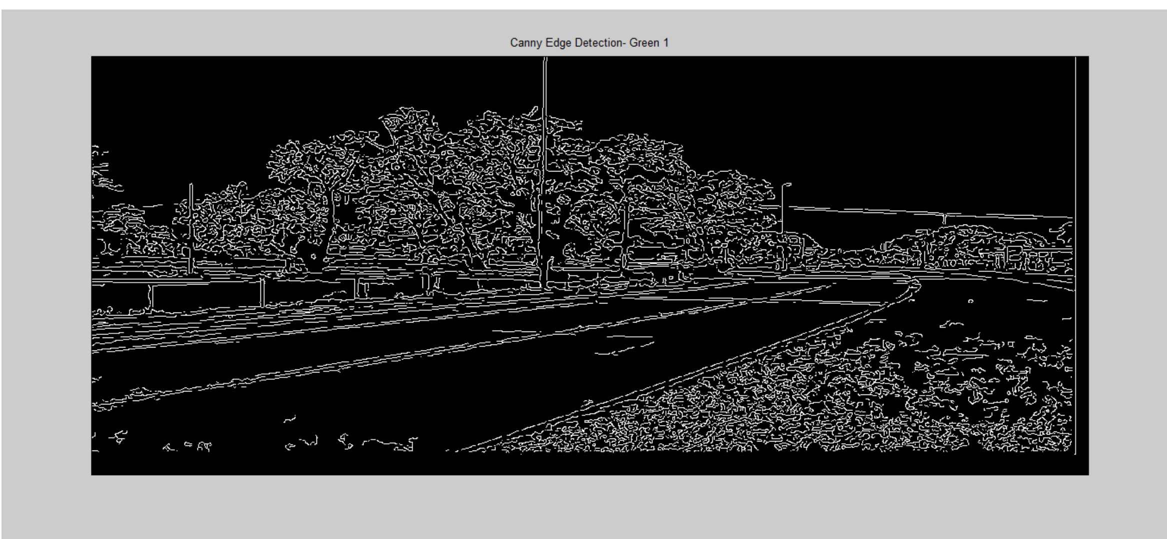

Figure 7: Shape-based segmentation using Canny Edge detector.

From the edge-based segmented image in Figure 7, the edge-oriented histogram is computed and plotted as shown in Figure 8. The edge-oriented histogram represents the count of the edge gradient (slope of each edge in image) in radians computed for an input image. These EOH features are important to represent the shapes of objects in GI designs, especially the shapes of trees.

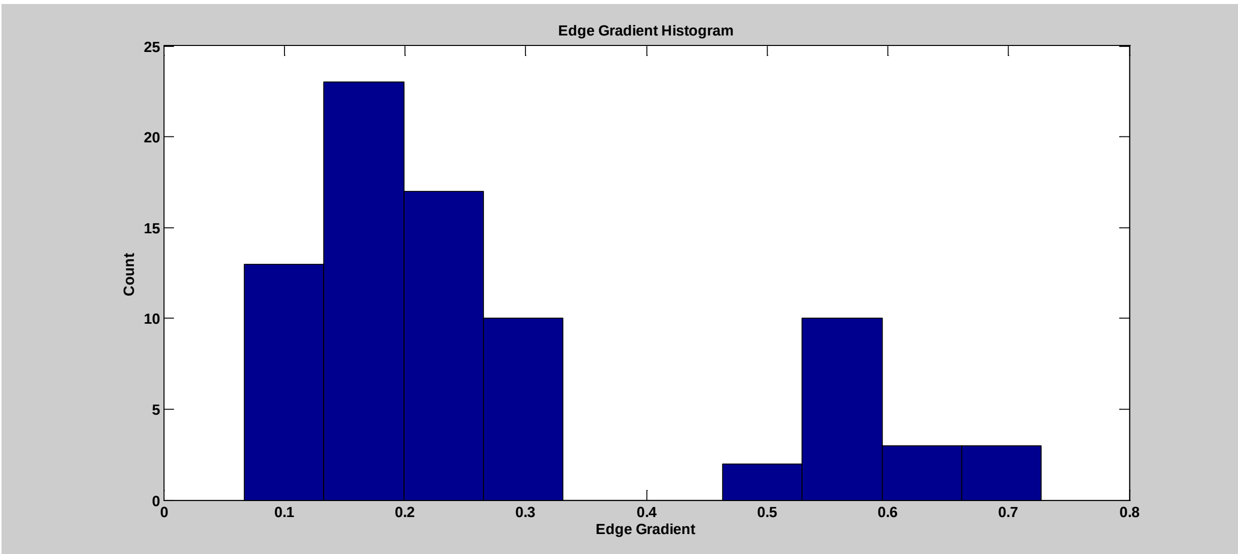

Figure 8: Edge Orientation Histogram.

2.1.4 Spatial Histogram:

Spatial histograms are higher order histograms that capture global spatial information by computing the frequency of locations of labeled pixels across all images (Birchfield and Rangarajan, (2005)). Every pixel in an image is associated with a label based on its similarity in characteristics such as color intensity, texture, etc. In this algorithm, color intensity has been used to determine the labels of each pixel across the image set. These label pixels are grouped together based on the similarity of intensity and their location is specified as the centroid of their cluster. This coordinate value is used to estimate the spatial information of similarly-labeled pixels in an image. The spatial histogram shown in Figure 9 (from the same input image as Figure 4) shows the frequency of bins that represent the mean spatial location of every labeled pixel in the image. In this manner, spatial histogram is capable of summarizing spatial information that is not represented with color histogram or edge-oriented histogram.

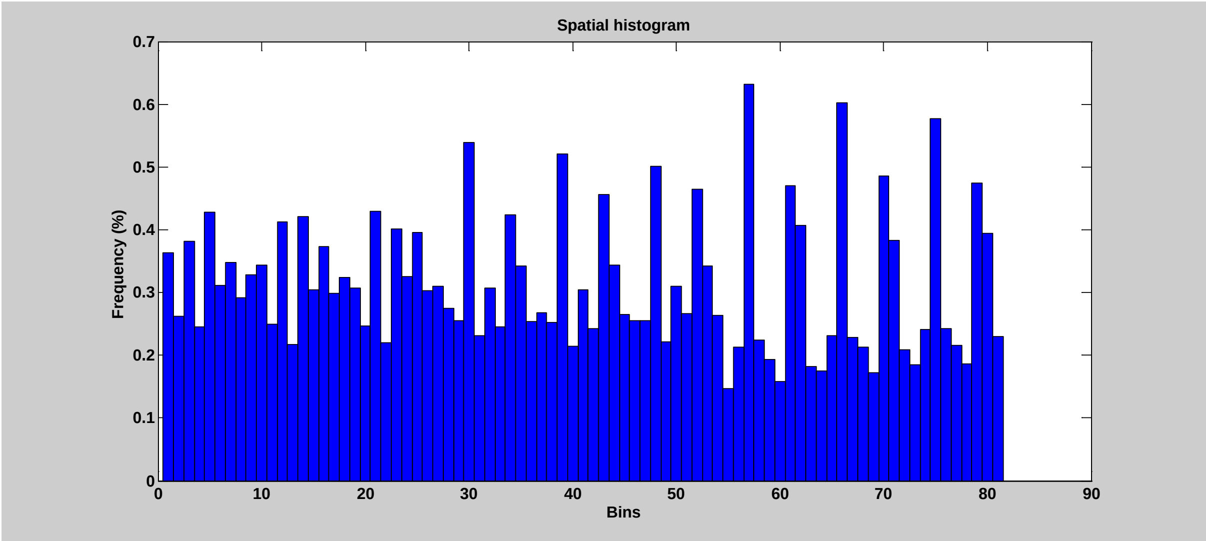

Figure 9: Spatial histogram for the image in Figure 4.

2.1.5 GIST Descriptor Features (Antonio, et al. 2001):

The previous two image features identify specific objects from the images. Antonio et al. (2001) proposed a technique to estimate the structure or shape of a scene using spatial properties of the scene, called GIST descriptors. The spatial properties of a scene are the composite set of boundaries in an environment, such as walls, sections, ground, elevation, and slant of the surfaces that define the shape of the space. The GIST descriptor identifies the dominant spatial structure of a scene (e.g., degree of naturalness, degree of openness, degree of roughness, degree of expansion). The mathematical model of the GIST descriptor implements principal component analysis for dimensional reduction of an input image (Wold, et. al., 1987). In this work, the GI input images are then modeled using the GIST descriptor algorithm called LMgist in Matlab. The GIST descriptors are computed by implementing the discrete Fourier transform (DFT) of an input image, which decomposes the image into its sine and cosine components. The output of the transformation represents the image in frequency domain, where each point represents a particular frequency contained by the pixel (Morgan, et al., (1991)). The DFT contains an amplitude function of frequency variables, which represents the energy spectrum or radiation in the image and provides information on the length and width of the contours that compose the scene.

Figure 10 shows the GIST descriptor for a sample input green space image. The results show the local energy spectrum, which measures the quantity of radiation passing through or emitted from the surface of an object, for the objects in the image, grouped spatially in a 4x4 matrix on the right side. Dark regions in the gist descriptor matrix (e.g., the upper right and lower left sub-images in Figure 10) represent the openness in the scenic image. Each sub-image of the 4x4 matrix corresponds to the amount of radiation (with multiple wavelengths) emitted or passed through objects placed in the corresponding spatial location. Objects such as the tree in the middle of the input image on the left in Figure 10 emits higher radiation and thus has more energy spectrum captured by the GIST descriptors in the corresponding sub-image. This spatial distribution of local energy spectrum helps in determining the holistic representation of a scene, such as the degree of openness/closeness that affect the complexity factor of the landscape as given in Table 1.

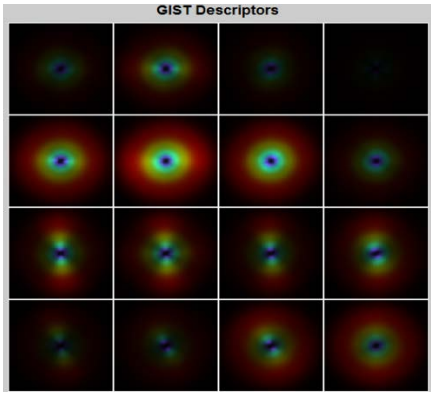

Figure 10: GIST Descriptor results for a sample image.

2.1.6 Machine Learning Model:

Once the GI design image features are extracted using the methods described above, a supervised machine learning approach is used to predict human preferences for each design. Supervised machine learning algorithms are used to learn or approximate some unknown or partially known function ($y=f(x)$) from a set of training data consisting of instances of the function's inputs and outputs (x, y). The output (y) can be discrete classes or labels – called a classification problem -- or can be continuous values -- called a regression problem. Once the model learns from the labeled training data, it is used to predict the outcome for any valid input. There are number of supervised machine learning algorithms -- see reviews by Mitchell, (1997) and Duda et.al, (2001). Predicting human preferences is a multi-class classification problem, where the training set consists of a group of images with human preference ratings on a scale of 1-5. The higher the rating, the more preferable is the GI design, as shown in the Figure 3.

In this research, the adaptive boosting algorithm is used to predict human preferences. Adaptive boosting (AdaBoost) is an ensemble learning algorithm, which combines a weak classifier such as decision trees or k-nearest neighbors (KNN) to output a strong classifier (Freund and Schapire, 1999). AdaBoost gives high accuracy and prevents over-fitting of parameters to the training dataset by using an iterative learning model, which improves accuracy by learning from mistakes made in an earlier training step. The algorithm continues iterating until its misclassification error falls below a user-specified threshold value. For this application, both decision trees and KNN were tested as the weak classifiers and decision trees performed best and were used in the results presented below.

2.2 Evaluating the hydrologic benefits of GI design:

In order to evaluate the hydrologic benefits of candidate GI designs, RHESSYS hydrologic model (Tague and Band, 2004) is used. RHESSYS is designed to simulate integrated water, carbon, and nutrient cycling and transport over spatially variable terrain at small to medium scales (i.e. from 1st to 3rd order watersheds). Its spatially distributed framework enables the modeling of spatiotemporal interactions between different eco-hydrological processes from patch to watershed scales (Hwang, et.al., 2012).

Figure 11 gives an overview of the steps involved in preparing the required input for GI simulation using RHESSYS and integrating it with the human preference model for social ranking. Google street view images are first extracted from the Google Maps application programming interface (API) (`http://maps.google.com`) for the neighborhood where GI design is planned. The coordinates (latitude/longitude) are identified using Google Maps for the front yard of every house in the neighborhood where GI installation is under consideration. These coordinates are used to generate patch identifications (ids) that are used as inputs for GI parameters in RHESSYS. Patch ids are unique numbers associated with particular ecosystem patches, which are the smallest-resolution spatial units that define areas of similar soil moisture and land-cover characteristics. In landscapes modified by humans, patches can also be defined to contain stream channels, road segments, storm sewers, etc. Human sources of water and nutrients are also defined at this level (Tague and Band, 2004). Therefore, adding trees to the existing patches requires reflecting the presence of trees in the existing lawn by generating patch ids from their respective coordinate values. Patch id numbers are generated using GRASS GIS (http://grass.osgeo.org), which queries the existing raster map layers to output labels associated with input coordinate values using the ‘r.what’ command. These labels are patch id numbers that represent the current vegetation type present in the raster map.

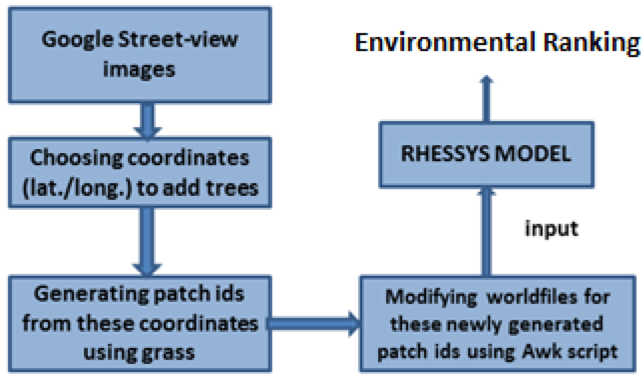

Figure 11: Framework of the steps involved in estimating GI hydrologic benefits using RHESSYS.

The next step in executing RHESSYS is to prepare additional non-spatial files, called worldfiles, which represent landscapes patterns like land use, tree canopy, etc. within RHESSYS. Worldfiles are generated with a GRASS interface program that references input raster maps and a text document defining initial state variables (e.g., saturation deficit within the patch level, which is a measure of the degree of saturation). Within the worldfile, each spatial layer is associated with the following identifiers: an assigned ID based on the map used and state variable values for stores and fluxes at each spatial level that are initialized at the start of the simulation. The *Grass2World* (g2w) program is used to generate the worldfiles automatically from spatial data layers within GRASS GIS. Next, in order to incorporate new trees into the existing worldfile based on the newly generated patch id numbers, an Awk script is used. Awk script is an interpreted programming language typically used for data extraction in UNIX operating systems (Alfred et.al, 1978).

Finally, the modified worldfile is used to execute the RHESSYS model and forecast the effects of the GI design on annual mean stream flow and base flow (Ritcher et.al, 1996) at the outlet of the urban catchment where the neighborhood is located. These statistics have previously been identified as important indicators for measuring the alteration in hydrology of an urban catchment due to changes in land use and land cover. By simulating the impacts of GI designs on mean flows using RHESSYS and comparing flows with current and pre-development values, we can observe the efficiency of the GI designs in moving towards restoration of pre-development urban watershed hydrology. This provides an initial environmental rating for the GI designs, which can be supplemented with nutrient impacts in the future.

Chapter 3

Case Study: Human Preference Model Validation in Galesburg, IL

The human preference model was trained and validated using images from Main Street in Galesburg, Illinois (training set), which were created by Professor William Sullivan's laboratory at the University of Illinois Urbana-Champaign.. The images were acquired from a standard digital camera of 8 megapixels. Some image features were modified using Adobe Photoshop simulates potential changes in particular green settings and record human preferences for each variation. The preferences were obtained by averaging ratings on a scale of 1 (least preferable) to 5 (most preferable) from 300 participants, and were used to train the supervised machine learning model presented in Section 2.1.7. Five-fold cross validation (Kohavi, 1995) was used to assess the accuracy of the machine learning model. Figure 11 shows examples from the validating set. The predicted ratings for each of these images were identical to the actual human ratings.

(a) Human Preference Rating: **2**

(b) Human Preference Rating: **4**

(c) Human Preference Rating: **1**

(d) Human Preference Rating: **3**

Figure 12: Example of validation results for Galesburg image data.

The overall prediction accuracy of the model is evaluated for both the training and testing sets as shown in Equation 1. Table 2 shows the results for both the training and validating image sets from Galesburg.

$$\textit{Prediction Accuracy (\%)} = \frac{Number\ of\ correctly\ classified\ image\ samples}{Total\ number\ of\ image\ samples}\ x\ 100 \qquad (1)$$

Table 2: Prediction Accuracy

Training set # 200 images	
Sample Set	Prediction Accuracy (%)
Training	96
Validation	74

The results indicate that the machine learning model predicts human preferences reasonably well, particularly since human ratings can have considerable uncertainty (James et al., 2009)

The training set is predominantly tree-based green infrastructure, and generally human preferences increase with more trees in images, as shown in Figure 12. However, merely adding more trees, bushes, plants, etc. are not sufficient to obtain high human preferences. The image features extracted from the training set (color histogram, EOH, spatial histogram, GIST descriptor), and their corresponding landscape features from Kaplan & Kaplan's preference matrix (1998), also play an important role.

For example, recall that color histogram and spatial histogram help measure the green coloring and coherence in the design. Figure 12 (c) and (d) show that the rating changes from 1 to 3 just by adding trees, which provides more green richness, and also by arranging the trees in an orderly manner along the sidewalks (i.e. Figure 12 (d) is more coherent than Figure 12 (c)). This added coherence can be seen in the color histogram results for these images in Figure 13.

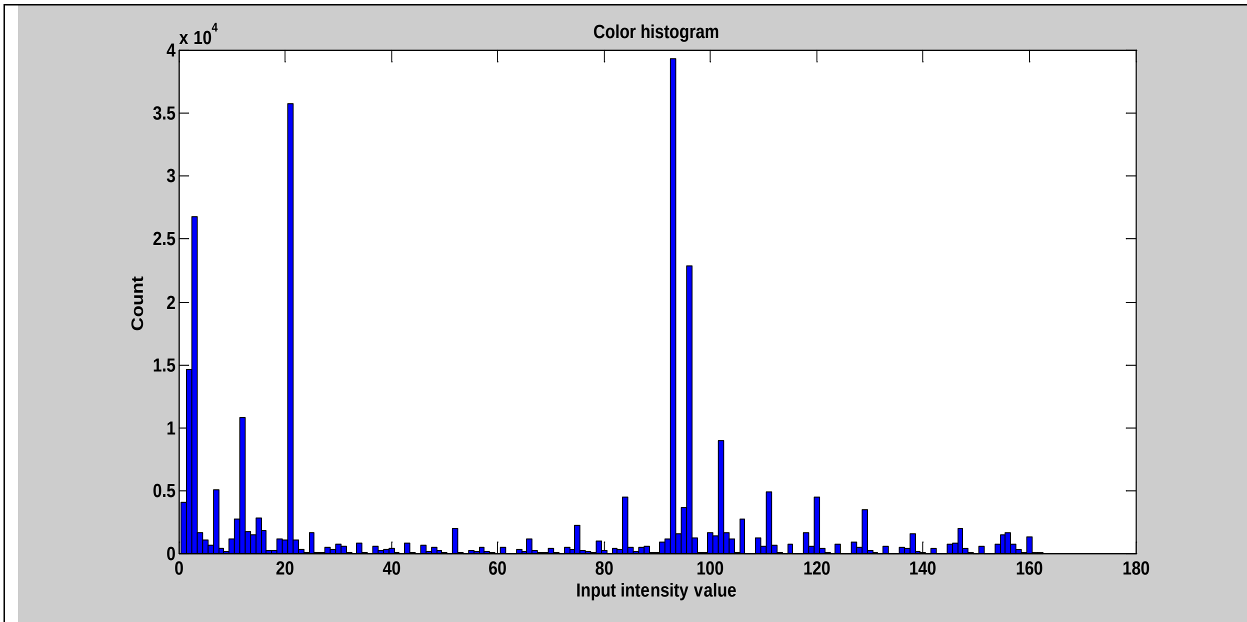

Color histogram for less coherent image in Figure 12(c)

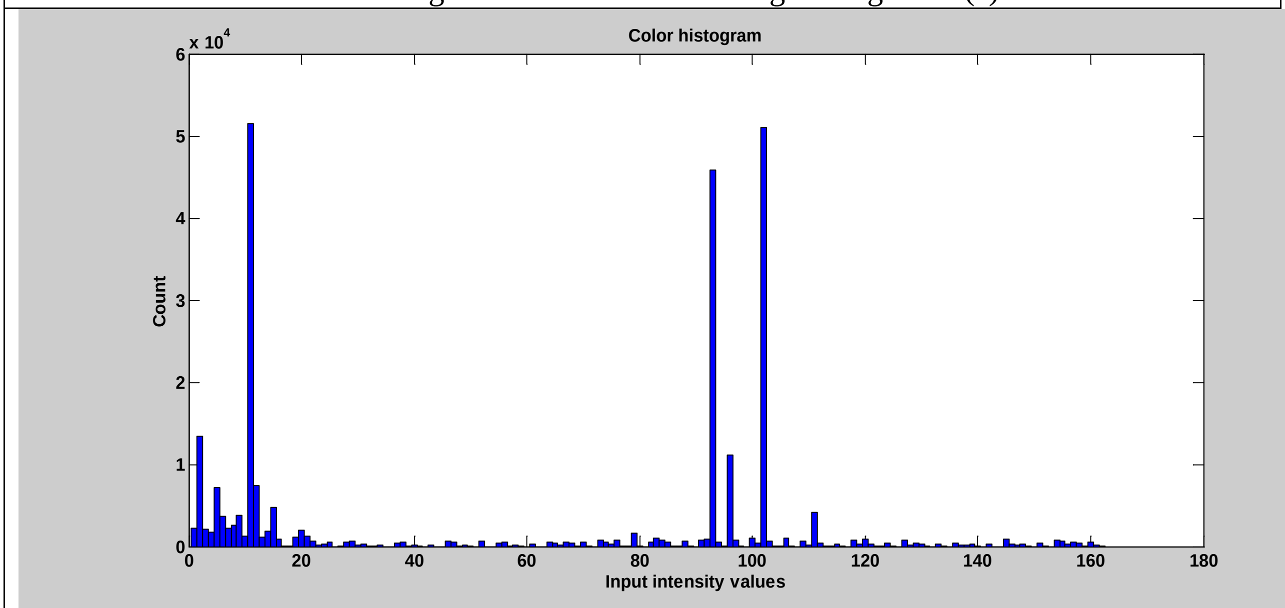

Color histogram for more coherent image with trees in Figure 12(d)

Figure 13: Comparison of color histograms showing increased coherence from adding trees.

The color histogram for Figure 12 (d) shows a different distribution of color intensity as compared to Figure 12 (c) due to the extra green color of trees added in Figure 12 (d).

Figure 12 (a) and (b) show how complexity, legibility, and mystery parameters of the preference matrix change human preferences. These parameters are captured by GIST descriptors, which show the amount of richness and degree of openness/closeness in an image, and edge oriented histogram (EOH), which reveals the shapes of objects in the image.

GIST Descriptors

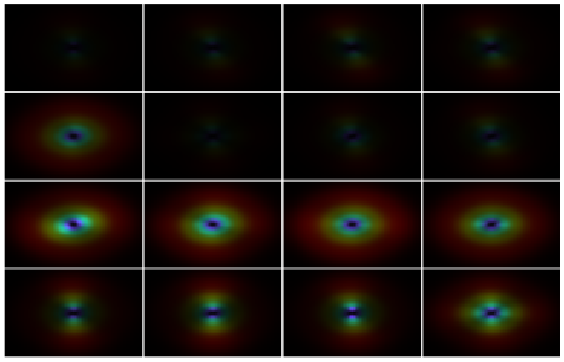

Figure 12(a)

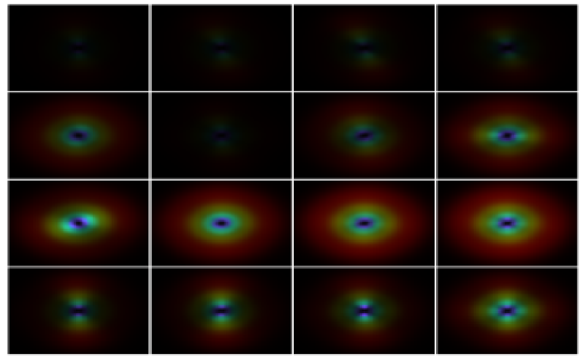

Figure 12(b)

EOH:

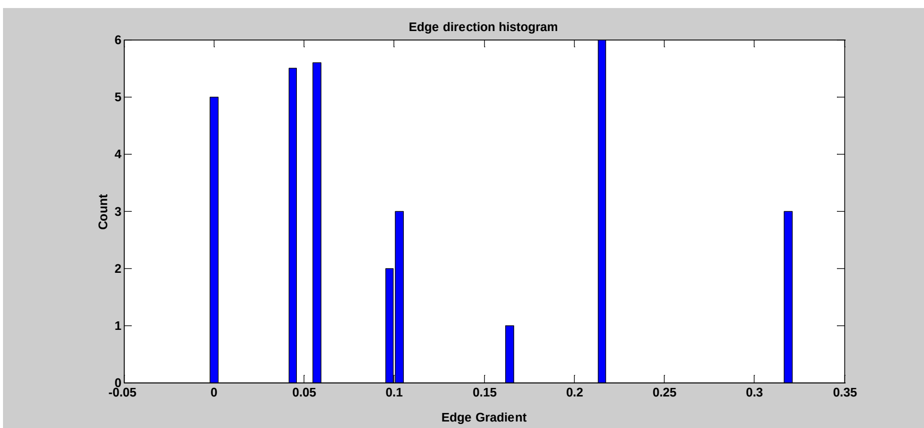

Figure 12(a)

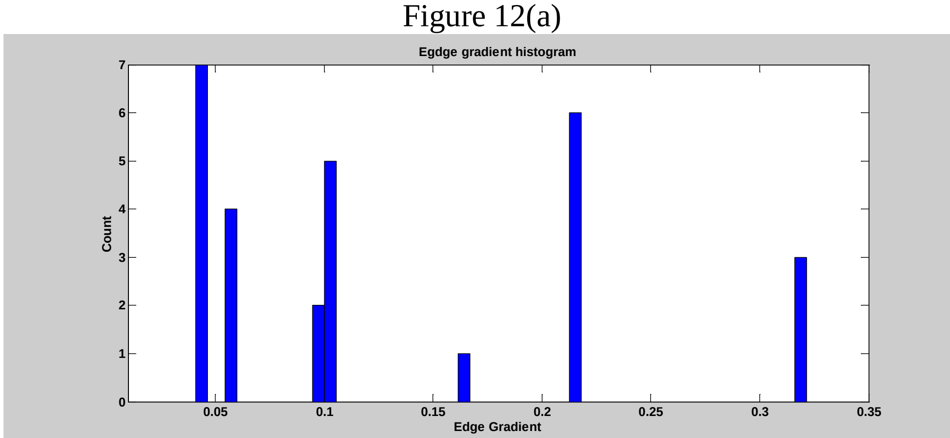

Figure 12(b)

Figure 14: GIST and EOH image features for Figures 12 (a) and 12 (b) reveal differences in complexity and legibility.

In Figure 14, note the variation in the GIST descriptors and edge oriented histogram for two different GI settings (Figure 12 (a) and (b)). The amount of richness and openness due to the presence of trees along the sidewalks in Figure 12 (b) is revealed in the increased energy spectrum in the upper right quadrant of the GIST descriptor. EOH indicates an increase in the count of edge gradients for trees in Figure 12 (b) as compared to 12 (a). Hence, both image features identify trees spatially located on both sides of the street and their shapes, which make the setting more legible, mysterious, and rich; hence Figure 12 (b) has higher preference than Figure 12 (a).

The results above show that the variability in human preferences for green spaces can be predicted based on image features that capture elements of Kaplan & Kaplan's preference matrix (1998). Given that hydrologic data and models were not available for Galesburg, IL, the next section examines how predicted human preferences align with hydrologic benefits of GI designs in Baltimore.

Chapter 4

Case Study: Implications for GI Design in Dead Run Watershed, Baltimore, MD

The GI design methodology described in Section 2 was applied in the Dead Run Watershed in Baltimore, MD, which is part of the Baltimore Ecosystem Study (BES). As the available training set for the GI model contains predominantly tree-based green infrastructure, the case study application focuses on adding trees in a neighborhood within Dead Run Watershed, shown in Figure 15, and observing how the human and hydrologic benefits change with different designs. Six scenarios were examined: 1) Existing scenario, 2) Adding a single tree in the neighborhood, 3) Adding multiple trees in open vs. clustered arrangements, 4) Adding small vs. large trees, 5) Adding trees on one vs. both sides of the street, and 6) Adding single vs. mixed species of trees.

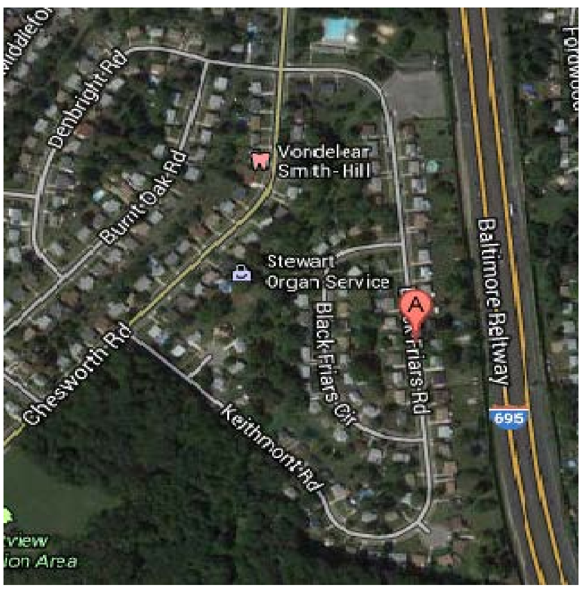

Figure 15: Map of Baltimore neighborhood examined for GI design.

Google Street-view images of the entire neighborhood were extracted and used as a base case for human preferences. The coordinate values (latitude & longitude) of the front yard of every house in the region were chosen as locations to add trees. Google Street-view overlay API javascript was used to overlay the trees in the Google image for modeling human preferences using the machine learning model trained and validated in Galesburg (Section 3). The results are given in Section 4.1.

Once the human preference ratings were obtained, RHESSYS was used to evaluate the hydrologic benefits of the added green infrastructure to the larger Dead Run Watershed using the methodology described in Section 2.2. The hydrologic data used in the simulations were collected by the Baltimore Ecosystem Study, as outlined by Band et al. (2007). The hydrologic impacts of the green infrastructure scenarios were compared with both the existing scenario, using 2007 hydrologic and model data from Band et al. (2007), and a pre-development scenario. The earliest hydrologic data available for the pre-development scenario is 1960, which was before the design neighborhood was built. The hydrologic results are presented in Section 4.2, along with a discussion of the interactions between human preferences and hydrologic benefits.

4.1 Results of Human Preference Modeling:

The human preference results for the six scenarios in Baltimore are shown below for a sample street view image

(a) Human Preference Rating: **2** (existing scenario)

(b) Human Preference Rating: **3** (one tree scenario)

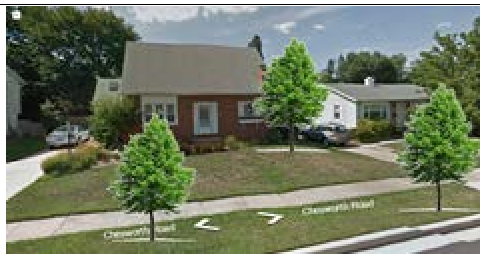

(c) Human Preference Rating: **3** (open arrangement with smaller trees)

(d) Human Preference Rating: **1** (clustered arrangement)

(e) Human Preference Rating: **4** (smaller trees on both sides)

(f) Human Preference Rating: **5** (larger trees on both sides)

(g) Human Preference Rating: **4** (open arrangement with larger trees)

(h) Human Preference Rating: **3** (open arrangement with mixed species)

Figure 16: Results of human preference modeling for different scenarios in Baltimore.

Settings that include trees, plants, bushes, etc. have been shown to reduce symptoms of both mental fatigue and stress (Coley et al. 1997; Sullivan et.al, 2004). The existing scenario (Figure 16(a)) lacks such a setting, and therefore the human preference model predicts a low rating. Simply by adding a single tree to the existing scenario (Figure 16(b)), the model predicts a higher preference rating based on shifts in the trained image features EOH and color histogram.

The spatial arrangement of trees in GI settings is also an important design factor that affects the level of complexity in the scene (Kaplan & Kaplan, 1989), which is captured in the model by the GIST descriptor feature. Highly complex settings are generally less preferable and thus the clustered arrangement of trees in Figure 16 (d) gets a much lower human preference rating than the open arrangement of trees in Figure 16(c). Figure 17 shows how this change is captured by shifting energy spectrums in the GIST descriptors.

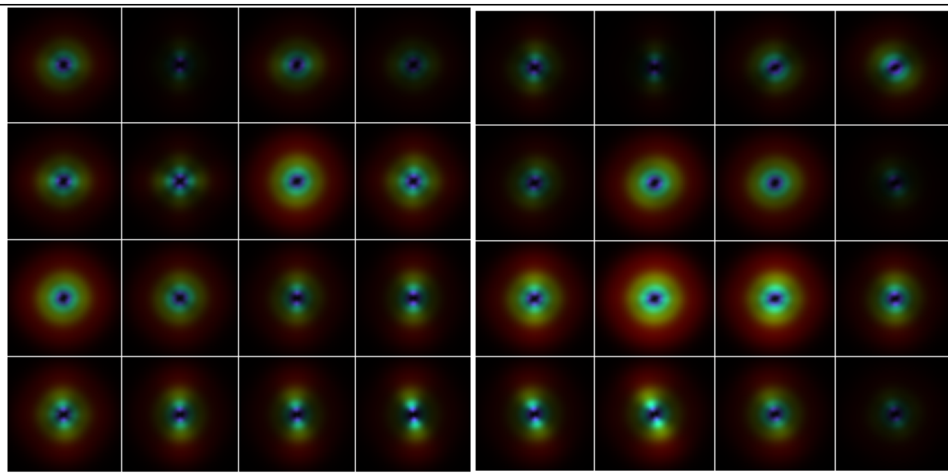

GIST descriptors for Figure 16(c)   GIST descriptors for Figure 16(d)

Figure 17: GIST descriptors reflect the increased complexity of clustered trees in Figure 16(d).

The legibility and mystery factors of human preference require three-dimensional inference, allowing people to imagine themselves in the scene (Kaplan and Kaplan, 1989). The mystery parameter involves exploration, and therefore the view of angle plays a very important role in human perceptions. The arrangement of trees on both sides of the street in Figures 16 (d) and (f) create a more three-dimensional view where people can imagine more exploration and thus prefer such settings. The human preference model is able to capture this parameter through shifts in all four image features (i.e., color histogram, spatial histogram, GIST descriptors, and edge orientation histogram), as shown in Figure 18. The spatial arrangement of trees on both sides of a street is well captured by the spatial histogram feature and tree shape and color are identified by color histogram and EOH. The visual change in GI setting, which encourages human beings to explore the setting, has been captured by all four features.

GIST descriptors

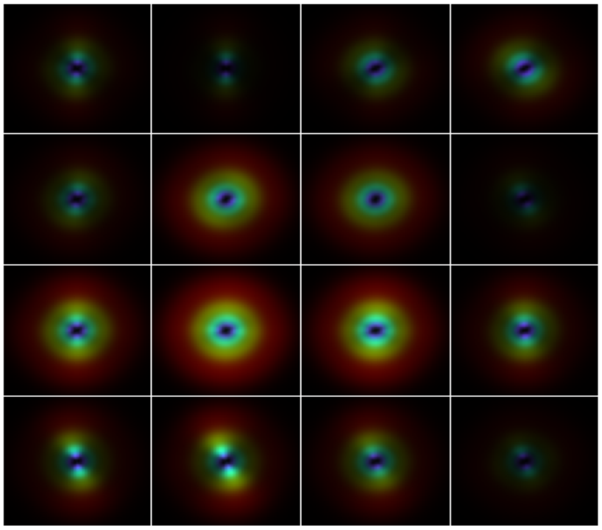

16(d)

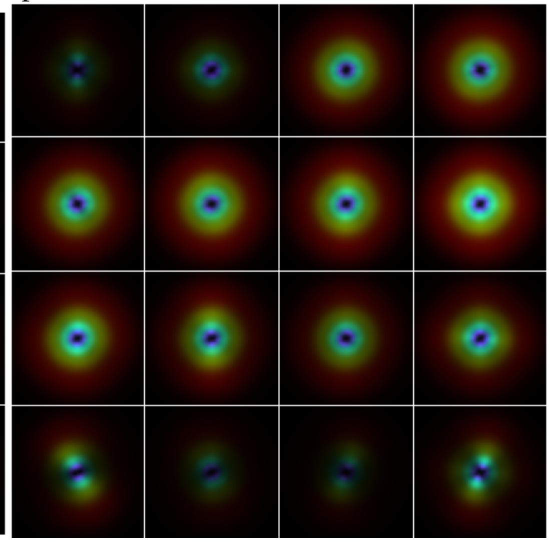

16(f)

Color histogram

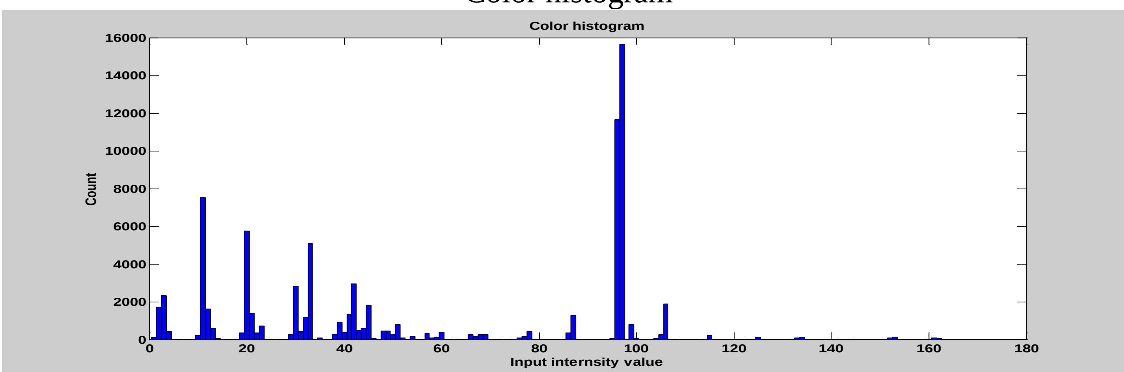

16(d)

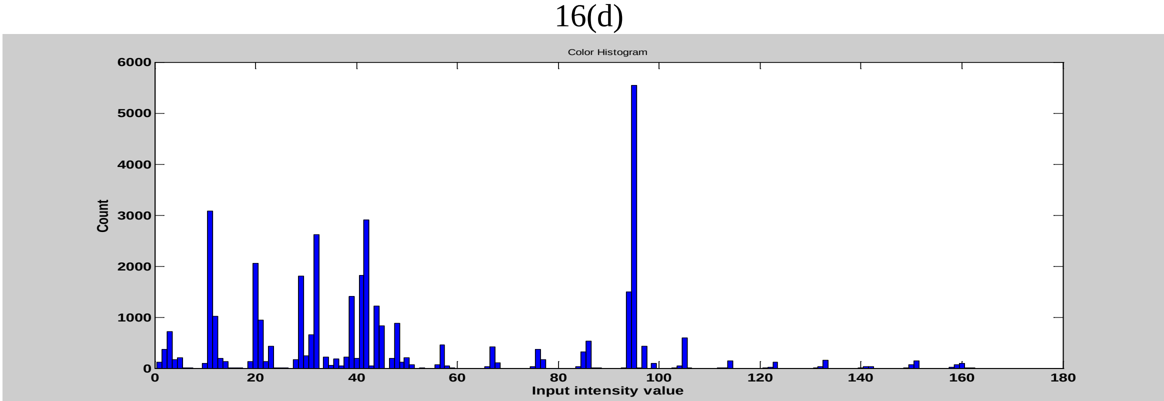

16(f)

EOH

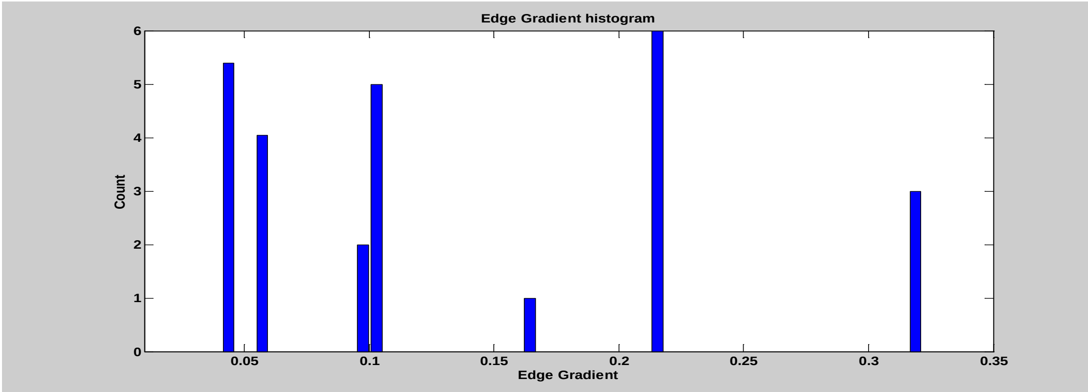

16(d)

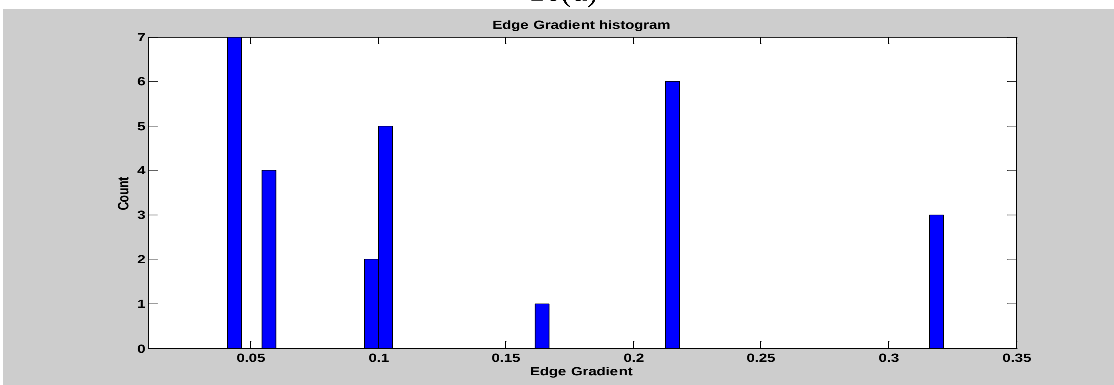

16(f)

Spatial histogram

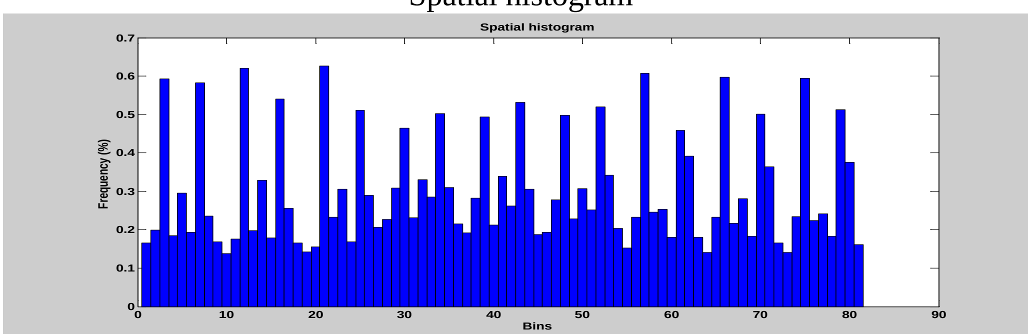

16 (d)

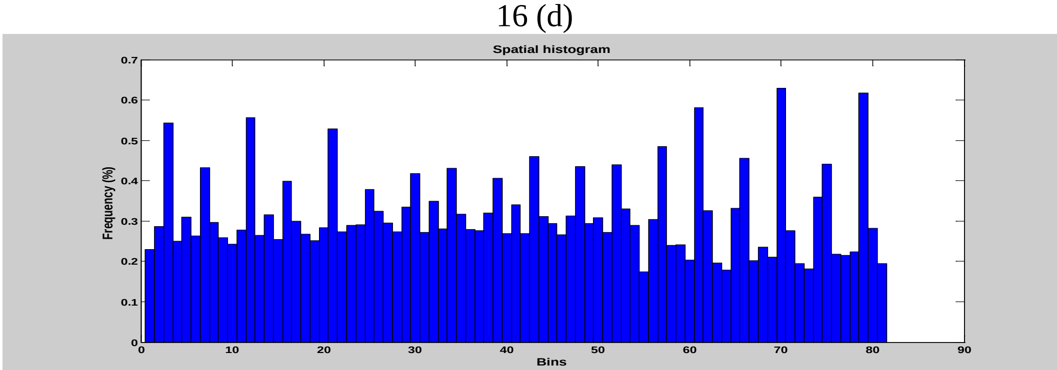

16(f)

Figure 18: Image features reflecting the change in visual appearance of setting.

Further, it is important to note that larger trees are more preferable than smaller trees and therefore have higher ratings (compare Figure 16(e) vs. (f), as well as 16(c) vs. (g)). The reason for this result is the higher degree of richness and complexity in the setting, which are captured by GIST descriptors. The degree of richness and complexity for a large versus small tree is shown in the GIST descriptors given in Figure 19. The setting with a large tree has fewer dark regions in the GIST matrix than the setting with a small tree.

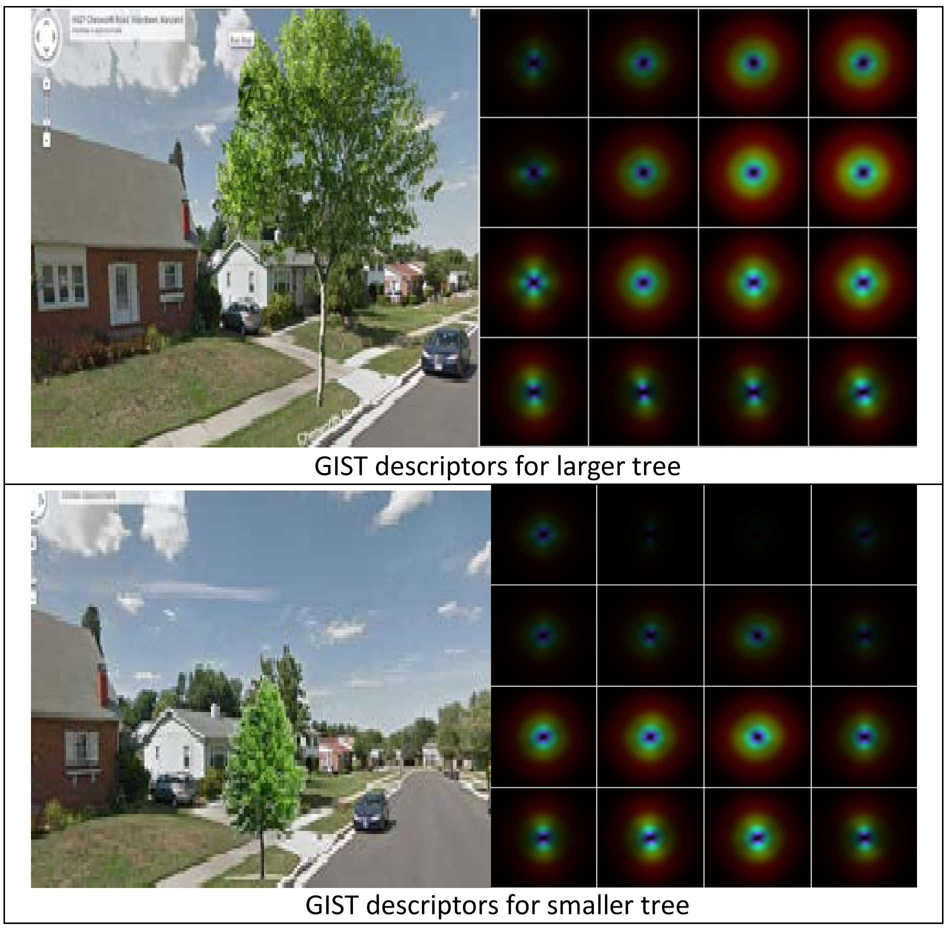

Figure 19: GIST descriptors for GI setting with a larger and smaller tree.

Another important factor affecting the preference ratings is coherence, which is achieved by having similar plant species and/or function and even distinguishable by other areas (Kaplan and Kaplan, 1989). People prefer having trees of the same species, and thus the arrangement of mixed species of trees (Figure 16(h)) has lower preference than similar trees (Figure 16 (g)), even though it is still an open arrangement. This perception is modeled by the color histogram and EOH, which capture how different species of plants have different shades of green color and distinct shapes.

4.2. Results of Hydrologic Modeling using RHESSYS:

The hydrologic impact of the GI design scenarios, given in Figure 20, compares the modeled change in annual mean stream flow and base (groundwater) flow for the following scenarios: 1) Existing condition (for the year 2007), 2), Pre-development conditions in 1960, 3) Adding a single tree to every yard in the neighborhood, and 4) Adding two trees to every yard in the neighborhood. Because hydrologic impacts are measured at the watershed outlet, the physical arrangement of the trees, which were important in the human preference results in Section 4.1, do not change the estimated hydrologic impacts.

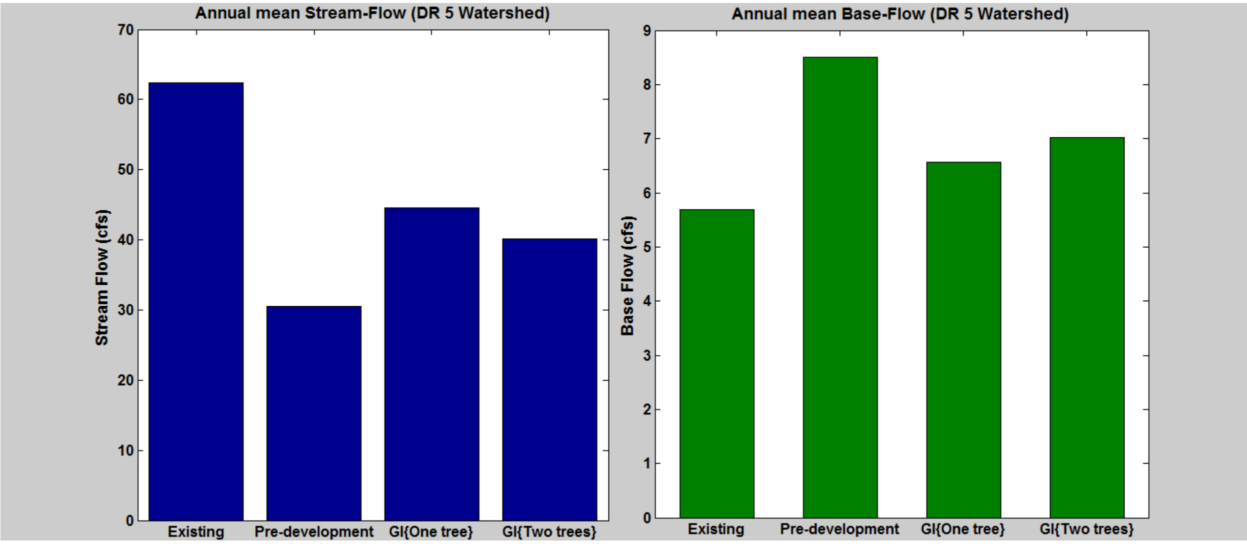

Figure 20: Hydrologic impacts of GI (trees) on annual mean stream and base flow in Dead Run Watershed.

The GI design scenarios significantly reduce the impacts of development on the urban watershed, shifting both the stream and base flows much closer to the pre-development scenario. The extent of the shift is particularly impressive given that the neighborhood of the GI design is only 1.2 percent of the land area in the overall Dead Run Watershed. The Dead Run Watershed has 36% of its land as impervious (Gwynn Falls water quality management plan, 2004), and thus adding more trees in front of every house in the neighborhood has significant beneficial impacts. Table 3 shows a quantitative comparison of the two different GI scenarios.

Table 3: Quantitative comparison of GI impacts for different scenarios

	Stream Flow Comparison		Base Flow Comparison	
GI Design Scenario	% reduction from existing scenario	% difference from pre-development scenario	% reduction from existing scenario	% difference from pre-development scenario
One tree (every yard)	26	32	15	23
Two trees (every yard)	36	46	23	17
Three trees (every yard)	36	46	23	17

From Table 3, it is clear that green infrastructure can play an important role in restoring the urban watershed to predevelopment hydrology. Adding two trees to every front yard in the neighborhood gives better results than one tree, but the incremental improvement declines as additional trees are added. In fact, adding three trees to every yard does not cause any additional changes to flow at the outlet of watershed. Moreover, the results in Section 4.1 indicate that the second and third trees in each yard do not cause significant differences in human preferences (compare Figures 16(b) and (d)), although their arrangements across the neighborhood are important.

The hydrologic benefits of adding more green components to urban watersheds helps in restoration of pre-development flows (US EPA, 2009), but our results also show that the human preference model can identify specific patterns for installing these green components that are more beneficial for human wellbeing.

Chapter 5

Conclusions

This work develops a novel computational green infrastructure (GI) design framework that couples storm-water management requirements with criteria for human wellbeing. Current approaches to designing green storm water features tend to emphasize rapid removal of storm water runoff to reduce impacts of downstream flows and pollutant loads. The approach presented in this paper is a first step towards incorporating the benefits of human wellbeing associated with these urban green spaces into the design process. In order to map landscape features that are correlated with human wellbeing to features that can be used to train a supervised machine learning model, a suite of computer vision algorithms and techniques have been used. The result is the first GI design model capable of predicting human preferences.

The results obtained from this research show that image mining and machine learning methods can reasonably predict human preferences for green infrastructure settings by capturing elements of Kaplan & Kaplan's landscape preference matrix. Variations in human ratings are reflected by shifts in the four image features used in this research, providing a new approach to rapidly screen potential GI designs along with hydrologic benefits.

However, in order to predict the human preferences for more green storm-water practices such as bioswales, rain gardens, cisterns, etc., a larger training set with images and human ratings of such designs are needed to train the machine learning model. The results also need to be validated with both hydrologic and human benefits measured at the same locations, including locations that span multiple hydroclimatic and socio-economic settings. This will help to identify how GI design benefits are affected by different settings.

However, in future, this integrated GI design approach could implement recommender system technique to measure the reliability of the system at new location. The recommender system would work on feedback loop system, where the predicted values of model would be cross verified by users living in that location.

Furthermore, in the future, advanced computer vision algorithms could be used to extract more local information from an image. For example, super-pixel segmentation techniques could be implemented to learn the exact shape of objects in an image (Fulkerson, 2007). Extracting the exact shape would help identifying the objects shape in image more accurately, and thus would improve the prediction accuracy of the model.

Furthermore, this type of human preference modeling can assist community stakeholders, storm-water engineers, and landscape designers in identifying specific features and arrangements of GI settings that attract more human beings and reduce their stress and anxiety, thus improving their health. Candidate designs can be pre-screened with the machine learning tool to identify a small set of promising designs that can then be evaluated by residents and other stakeholders. Emerging technologies, such as model-as-a-service (Santos, (2003)) and social networking, enable interactive use of the models and ratings of candidate designs through simple Web browser interfaces. As more design ratings are gathered, the accuracy of the human preference predictions will improve over time and the machine learning model can easily be re-trained. This type of interactive, stakeholder-driven design process offers promise for reducing concerns that environmental design for efficiency alone can lead to unsustainable solutions and stakeholder resistance (Ostrom, 2007; Ostrom et al., 2007; Brock and Carpenter, 2007).

References:

Alfred, V.A., Brian, W.K., & Peter, J. W (1987). The AWK programming language. Addison-Wesley Longman Publishing Co., Inc. Boston, MA, USA © ISBN:0-201-07981-X .

Anami, B. S., Nandyal, S. S., & Govardhan, A. (2010). A combined color, texture and edge features based approach for identification and classification of indian medicinal plants. International Journal of Computer Applications IJCA, 6(12), 45-51.

Bettez, N. D., & Groffman, P. M. (2012). Denitrification potential in stormwater control structures and natural riparian zones in an urban landscape. *Environmental Science and Technology*, *46*(20), 10909-10917.

Bettez, N. D., & Groffman, P. M. (2012). Denitrification potential in stormwater control structures and natural riparian zones in an urban landscape. *Environmental Science and Technology*, *46*(20), 10909-10917.

Caltrans Storm Water Quality Handbooks Project Planning and Design Guide, July 2010.

Canny, J. (1986). A Computational Approach to Edge Detection. *IEEE TRANSACTIONS ON PATTERN ANALYSIS AND MACHINE INTELLIGENCE, VOL. PAMI-8, NO. 6*

Chang, C.Y., Chen, P.K. (2005). Human response to window views and indoor plants in the workplace. *Hortscience, 40*(5), 1354-1359.

City of Portland Stormwater Management Manual, Revision 4, August 2008

Dash, M., & Liu, H. (1997). Feature selection for classification. *Intelligent data analysis*, *1*(1-4), 131-156.

Dietz, M. E. (2007). Low impact development practices: A review of current research and recommendations for future directions. Water, Air, & Soil Pollution, 186(1), 351-363.

Douglas, I. (2004). Urban greenspace and mental health.UK MAB Urban Forum.

Dalal, N. and Triggs, B. (2005): Histograms of Oriented Gradients for Human Detection. *Computer Society Conference on Computer Vision and Pattern Recognition. IEEE*

Duda, R. O., Hart, P.E., and Stork, D.G. (2001), *Pattern Classification*, (2nd Edition),
Freund, Y and Schapire, R.E (1999): A short Introduction to Boosting. *Journal of Japanese Society for Artificial Intelligence, 14(5):771-780.*

Fulkerson, B., Vedaldi, A., and Soatto, S. (2007). Class Segmentation and Object Localization with Superpixel Neighborhoods.

Harper, H.H. & Baker, D.M. (2008). Evaluation of Current Stormwater Design Criteria within the State of Florida, prepared for Florida Department of Environmental protection, Contract FDEP S0108.

Hartigan, J.A. (1975): Clustering Algorithms. *99th John Wiley & Sons,* Inc. *New York, NY, USA ISBN:047135645X*

Hwang, T., L. E. Band, J. M. Vose, and C. Tague (2012), Ecosystem processes at the watershed scale: Hydrologic vegetation gradient as an indicator for lateral hydrologic connectivity of headwater catchments, Water Resour. Res., 48, W06514, doi:10.1029/2011WR011301.

James et.al., (2009). Towards an integrated understanding of green space in the European built environment. *Urban Forestry & Urban Greening, Volume 8, Issue 2, Pages 65-75.*

Jessica Santos, (2003) "E-service quality: a model of virtual service quality dimensions", Managing Service Quality, Vol. 13 Iss: 3, pp.233 - 246

Kohavi, R (1995). A Study of Cross-Validation and Bootstrap for Accuracy Estimation and Model Selection. Appears in the International Joint Conference on Artificial Intelligence (IJCAI).

Lee, G.L., A. Selvakumar, K. Alvi, J. Riverson, J.X. Zhen, L. Shoemaker, F.

Lai 2012. A watershed-scale design optimization model for stormwater best management practices. Environ. Modelling and Software, 37, 6-18.

MacQueen, J. B. (1967), Some Methods for classification and Analysis of Multivariate Observations, *Proceedings of 5-th Berkeley Symposium on Mathematical Statistics and Probability*, Berkeley, University of California Press, 1:281-297.

MDE (Maryland Department of the Environment) Water Management Administration (2009). Stormwater Design Manual Volumes I & II.

Mitchell, M. T. (1996), *Machine Learning*, McGraw Hill, New York.

Mitchell, R. & Popham, F. (2008). Effect of exposure to natural environment on health inequalities: an observational population study. *Lancet* 372: 1655–60.

Morris, N. (2003). OPENspace: The research center for inclusive access to outdoor environments, 2003.

NRC 2008. Committee on Reducing Stormwater Discharge Contributions to Water Pollution, Water Science Technology Board 2008. "Urban Stormwater Management in the United States" National Academies Press, 513p.

NCDWQ (North Carolina Division of Water Quality) (2007) Stormwater Best Management Practices Manual (July 2007).

Ostrom, E. (2007). A diagnostic approach for going beyond panaceas, *Proceedings of the National Academy of the Sciences of the United States of America, 104*(39), 15181-15187.

Ostrom, E., Janssen, M.A., & Anderles, J.M. (2007). Going beyond panaceas, *Proceedings of the National Academy of the Sciences of the United States of America*, *104*(39), 15176-15178.

Dunn, A. D. (2010). Siting green infrastructure: legal and policy solutions to alleviate urban poverty and promote healthy communities. BC Envtl. Aff. L. Rev., 37, 41.

Pataki, D. E., Carreiro, M. M., Cherrier, J., Grulke, N. E., Jennings, V., Pincetl, S., & Zipperer, W. C. (2011). Coupling biogeochemical cycles in urban environments: ecosystem services, green solutions, and misconceptions. Frontiers in Ecology and the Environment, 9(1), 27-36.

Kaplan, R., & Kaplan, S. (1989). *The experience of nature: A psychological perspective*. Cambridge University Press.

Vailaya, A., Jain, A., & Zhang, H. J. (1998). On image classification: City images vs. landscapes. *Pattern Recognition*, *31*(12), 1921-1935.

Wendel , H. E. W., Downs, J. A., & Mihelcic, J. R. (2011). Assessing Equitable Access to Urban Green Space: The Role of Engineered Water Infrastructure. *Environmental Science and Technology*, *45*, 6728–6734 Wiley-Interscience.

Wold, S., Esbebsen, K., & Geladi, P. (1987). Principal Component Analysis. *Chemometrics and Intelligent Laboratory Systems, 2 (1987) 37-52.*

Wong, T.H.F., H.P. Duncan, T.D. Fletcher, and G.A. Jenkins. (2001). A Unified Approach to Modeling Urban Stormwater Treatment. *In Proceedings of the Second South Pacific Stormwater Conference.*

Wu, M.N, Lin, C.C., & Chang, C.C. (2007). Brain Tumor Detection Using Color-Based K-Means Clustering Segmentation. *IEEE Transactions on Image Processing.*